CBED Phase And Symmetry Determination Of A New Member Of Homologous Series $Ga_2O_3(ZnO)_{10}$

Emile D. Tchouankwe Kamga*, Werner Mader, C.M. Kede*, Luc Mbaze Meva'a* and Armin Kirfel*****

*Department of chemistry, University of Douala, BP. 24157 Douala Cameroon

**Institute of inorganic chemistry, Department of inorganic material research, university of Bonn

***Institute of mineralogy, Department of crystallography, university of Bonn

The phase and symmetry determination of $Ga_2O_3(ZnO)_{10}$, gallium zinc oxide, are presented by the means of CBED (convergent beam electron diffraction) technique. After synthesized the crystal, the scanning electron microscope pattern shows the orthorhombic shaped crystal. Using the determined main crystallographic axes [100], [010] and [001], the cell parameters have been proved to be a=3.32, b=19.45, c=36.55 Å, and $\alpha=\beta=\gamma=90^{\circ}$. Since the crystal shows large lattice parameters, the LACBED (large angle convergent beam electron diffraction) combined with the CBED method has been used to determine the point group. This combination has successful showed that the space group of $Ga_2O_3(ZnO)_{10}$ is **Cmcm**.

1. Introduction

The hexagonal Zinc Oxide has found applications in the manufacturing of different devices such as ultrasonic signal converters, oxygen sensors, chemical sensors and piezoelectric materials (C. Campbell et al., 1989; H. Cao et al., 2000; D. S. Ginley et al., 2000). Pure Zinc oxide is an n-type semiconductor with a band gap of 3.37 eV and a specific resistance of about 300Ω.cm. This specific resistance can be considerably influenced by the doping of ZnO with Li^{+}, Al^{3+}, Ga^{3+} etc. (Minami et al. 1984; Y. G. Wang et al. 2003). The homologous series, compound with long period, arise from the doping of the ZnO with an exceeding amount of trivalent metal ions, which can replace the divalent Zn ion but can not retain the wurtzite structure (Yuichi Michiue et al. 2012). Since the ZnO materials are candidates for photocatalysts (Kudo & Mikami, 1998), transparent conducting oxides (Moriga et al. 1998) and thermoelectric materials (Ohta et al., 1996), studies have been extensively carried out for the homologous phases $In_2O_3(ZnO)_m$ (Kasper, 1967) and related compounds. Further structural Studies of homologous phases revealed that the structures of $Fe_2O_3(ZnO)_m$ are the superstructures of $In_2O_3(ZnO)_m$ (Kimizuka et al. 1993). Furthermore, The homologous phases $InMO_3(ZnO)_m$, which is isostructural with $In_2O_3(ZnO)_m$, are found in systems In_2O_3-M_2O_3-ZnO(M= Fe, Ga, Al) (Kimizuka et al. 1989). High resolution microscopy and single crystal X-ray studies showed that the structure of $Ga_2O_3(ZnO)_m$ is fundamentally different from that of $In_2O_3(ZnO)_m$ type (Kimizuka et al., 1995; Michiue et al., 2008; Michiue & Kimizuka, 2010).

The unit cell of new homologous phase $Ga_2O_3(ZnO)_{10}$ was determined by the CBED technique by using the small camera length. Therefore, the ensuing 3D information have been taken into account: the diameter of FOLZ (first order laue zone), the relative distances of reflections in the FOLZ compared with reflections in the ZOLZ (zero order laue zone) and the relative positions of reflections in the FOLZ compared with reflections in the ZOLZ (Raghavan Ayer, 1989; Steeds, J. W., 1980; J.M. Zuo, 1989). Furthermore, point group and space group were determined by combining the CBED with LABED method (Michiyoshi Tanaka, 1986; Michiyoshi Tanaka et al., 1980).

2. Experimental

Metal Oxide Powder in molar ratios ZnO : Ga_2O_3 = 1 : 10 (Sigma Aldrich, 99.99%), were mixed in a ball milling with ethanol. The sample was dried, sealed in a Pt tube, put into the furnace at 873 K. The temperature was automatically increased with a heating rate of 278 K/min until the annealing temperature of 1632 K has been reached, and the sample stand in the furnace during 2 weeks. Thereafter, the samples was slowly cooled and taken out of the furnace at 773 K. It outcomes light yellow to yellow metallically shining single crystals, which had formed aggregates.

The phase stability of synthesized single crystals was examined by measuring the XRD on scanning electron microscope Philips XL20. Convergent Beam Electron Diffraction (CBED) and Large Angle Convergent Beam Electron Diffraction (LACBEB) were carried out on Phillips EM 400 and CM 30 with camera length respectively equals 4.543 and 3.720 mmÅ.

3. Results

3.1. Lattice constants

CBED patterns supplie 2D projections of 3D reciprocal lattice and can be used for determining the lattice parameters. The important factor for determining the lattice constants is the diameter of FOLZ-ring, which can be used to measure the distance between the reciprocal lattice plans parallel to electron radiation (Raghavan Ayer, 1989; Steeds, J. W., 1980; J.M. Zuo, 1989).

A simple geometrical relation under consideration of Ewald construction leads to:

$$G^2 = (2/\lambda - H)H$$

Where G is the radius of FOLZ in reciprocal space and H the distance between the plan of reciprocal lattice. In real space the above equation becomes:

$$H^* = 2/\lambda G^2 = 2/\left(\lambda \bullet (R/CL)^2\right)$$

Where $H^* = 1/H$ is the transformed, measured distance between ZOLZ und FOLZ in real space, R is the measured Radius of FOLZ in diffraction diagram and CL the camera constant. In the case of primitive orthorhombic crystal system the above equation becomes:

$$H^* = \left(a^2m^2 + b^2n^2 + c^2o^2\right)^{1/2}$$

With [mno] the crystallographic zone axis parallel to electron radiation. By setting the zone axes [100], [010] and [001] in the combination of above mentioned equations, the lattice constants can be calculated by the ensuing equations:

$a = 2/\left(\lambda \bullet (R_1/CL)^2\right)$, $b = 2/\left(\lambda \bullet (R_2/CL)^2\right)$ and $c = 2/\left(\lambda \bullet (R_3/CL)^2\right)$

Since the FOLZ Ring depends on both the dynamic and the cinematic scattering, the crystal has been investigated with different accelerating voltages 120kV and 300kV. The figure 1 shows the crossing Kikuchi-bands which define the zones axes and show the FOLZ-Ring. The used camera length, camera constants and the calculated lattice constants are listed in the table 1.

Table 1. Calculated lattice constants and for it used parameters

Parameters		[mno]
R_1(mm)	20.25	[100]
CL(mmÅ)	4.543	
λ_{120}(Å)	0.030285714	
a(Å)	3.32	
R_2(mm)	8.5	[010]
CL(mmÅ)	3.720	
λ_{300}(Å)	0.019699551	
b(Å)	19.45	
R_3(mm)	6.20	[001]
CL(mmÅ)	3.720	
λ_{300}(Å)	0,019699551	
c(Å)	36.55	

Figure 1. CBED-WP patterns of zone axes [100] taken with an accelerated voltage at 120kV, [010] and [001] taken at 300kV.

3.2. Bravais Lattice

The comparison of relative distance and relative position of reflections in FOLZ with reflections in ZOLZ has particular signification in the determination of Bravais lattices. In the case of primitive crystal rows of FOLZ reflections always continue corresponding to the positions of ZOLZ reflections along crystallographic zone axis, whereas in the case of centring of lattice FOLZ reflections are shifted and take places in the middle between ZOLZ reflections (Raghavan Ayer, 1989).
Comparative observations in the figure 2 show that rows of FOLZ reflections always continue corresponding to the positions of ZOLZ reflections along the crystallographic zone axis [001], whereas along [010] FOLZ reflections are shifted and take places in the middle between ZOLZ reflections. Therefore, the investigated phase is a **C**-centred Lattice.

3.3. Point group

For determining the point group the high symmetry zone axis has been chosen because low symmetry zone axis shows only small number of symmetry elements in CBED patterns. Since the calculated lattice parameters were large, the diameter of diffraction disk is accordingly too small. In this case, the intensity repartition of reflections can not clearly reflect the symmetry of crystal. The unique solution to solve this problem is the application of LABED technique which allows the symmetry determination in BF-Pattern (bright field) (Michiyoshi Tanaka et al., 1983, 1989, 1994; Buxton et al., 1976; Pogany et al., 1968; Goodman, 1975; Goodman et al., 1968; Bird, 1989).
Figure 3 and 4 show left the WP pattern (whole pattern) and rights the BF pattern of the zone axes [001] and [010] respectively. In the WP and BF pattern the projection group $\mathbf{2m_V m_{V'}}$ can obviously be observed.
The apparitions of supplement reflections in the FOLZ, which are forbidden in the ZOLZ, are conditioned by one sliding mirror plane perpendicular to the zone axis (Raghavan Ayer, 1989: J. W. Steeds et al., 1983).
When observing the CBED pattern of figure 6, the ensuing forbidden reflections 1147, 1149, $11\bar{4}\bar{7}$, $11\bar{4}\bar{9}$, $\bar{1}147$, $\bar{1}149$, $\bar{1}\bar{1}\bar{4}\bar{7}$ and $\bar{1}\bar{1}\bar{4}\bar{9}$ appear in the FOLZ. These were given rise by the sliding mirror plane perpendicular to the zone axis [010]. Furthermore, this observation agrees the presence of horizontal sliding mirror plan $\mathbf{21_R}$ and the resulted diffraction group $\mathbf{2mm1_R}$. According to the table 2, table of Buxton et al. 1976, the point group has been deducted and is **mmm.**

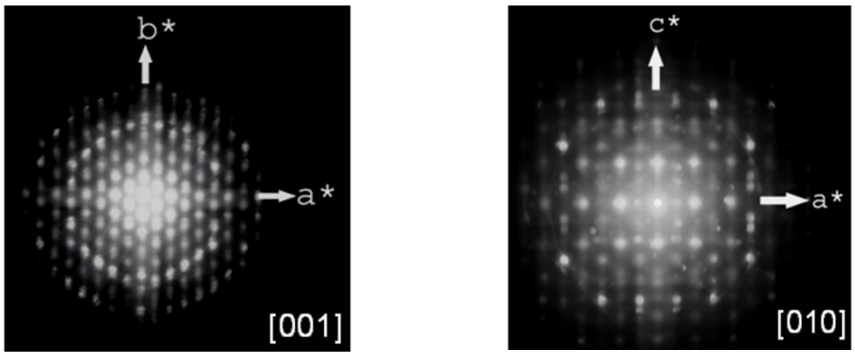

Figure 2. CBED patterns of zone axis [001] and [010] taken at 300kV show the ZOLZ and FOLZ

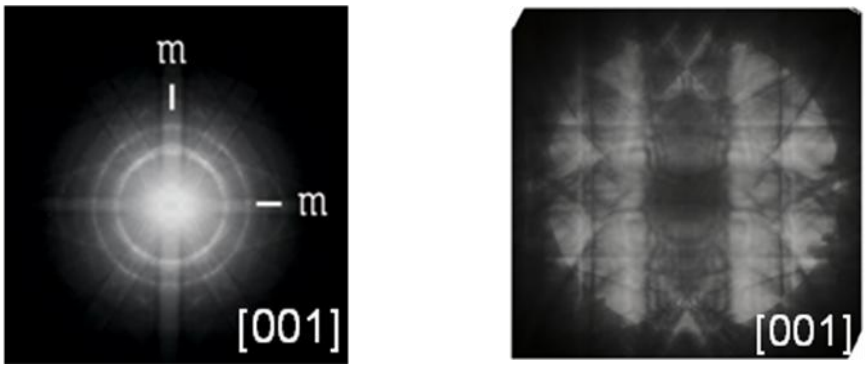

Figure 3. CBED-WP and LACBED-BF pattern of zone axis [001].

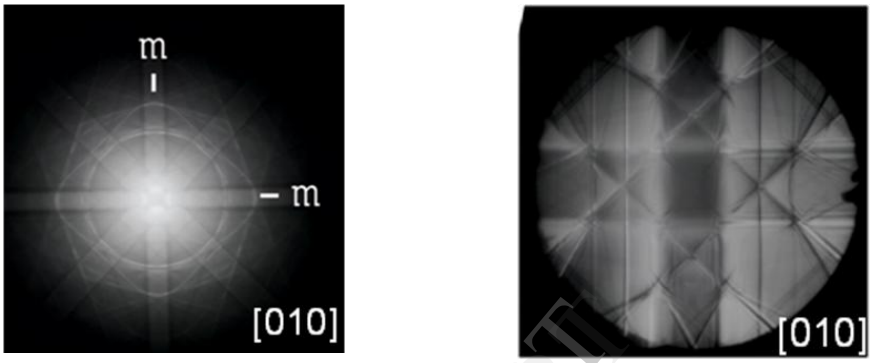

Figure 4. CBED-WP and LACBED-BF pattern of zone axis [010].

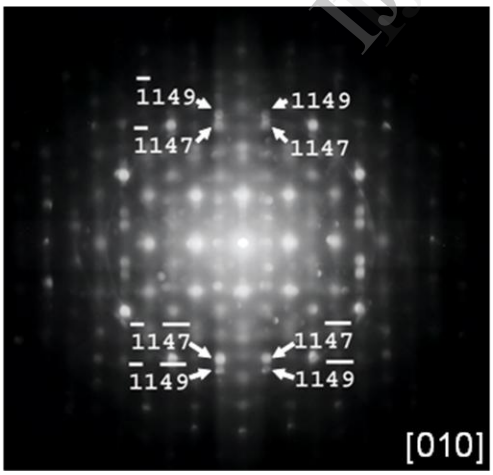

Figure 5. CBED pattern of zone axis [010] showing the forbiden reflections in the FOLZ.

Table 2. Relation between diffraction group and crystal point group from Buxton et al.(1976)

Diffraction Group	Point Group: 1	$\bar{1}$	2	*m*	2/*m*	222	*mm*2	*mmm*	4	$\bar{4}$	4/*m*	422	4*mm*	$\bar{4}2m$	4/*mmm*	3	$\bar{3}$	32	3*m*	$\bar{3}m$	6	$\bar{6}$	6/*m*	622	6*mm*	6*m*2	6/*mmm*	23	*m*3	432	$\bar{4}3m$	*m*3*m*
$6mm1_R$																										x						
$3m1_R$																									x							
$6mm$																								x								
$6m_Rm_R$																							x									
61_R																						x										
31_R																					x											
6																				x												
6_Rmm_R																			x													x
$3m$																		x													x	
$3m_R$																	x													x		
6_R																x													x			
3															x													x				
$4mm1_R$														x																		x
4_Rmm_R													x																		x	
$4mm$												x																				
$4m_Rm_R$											x																			x		
41_R										x																						
4_R									x																							
4								x																								
$2mm1_R$							x								x											x		x				x
2_Rmm_R					x			x			x				x					x			x			x		x				x
$2mm$						x																			x							
$2m_Rm_R$							x					x		x										x			x		x			
$m1_R$								x					x	x											x	x					x	
m				x				x					x	x					x			x			x	x					x	
m_R			x			x	x		x	x		x	x	x				x			x			x	x	x		x		x	x	
21_R					x															x												
2_R		x			x			x			x				x		x			x			x				x		x			x
2			x															x														
1_R				x															x													
1	x		x	x		x	x		x	x		x	x	x		x		x	x		x	x		x	x	x		x		x	x	

3.4. Space group

The screw axes and the sliding mirror planes lead to forbidden reflections in the cinematic diffraction. Cinematic forbidden reflections can be exited with considerable intensity under the condition of dynamic scattering if the conditions of Umweganregung and Bragg criteria are sufficiently well satisfied. However, such reflections appear in CBED patterns because of multiple scattering paths as lines of absence (dark bars) or Gjonnes-Moodie lines within disks of limited intensities (J. GjØnnes et al.,1965; Cowley et al., 1959; M. Tanaka et al., 1983, 1985, 1988; P. Goodman et al., 1980; J. M. Howe, 1986).

It outcomes from the observation of CBED pattern of figure 6 that the G-M lines, which appear in the reflections ***00l*** (with ***l*** uneven) of FOLZ rings, are perpendicular to [100], [010] and parallel to [001]. From the G-M lines table of Tanaka et al. 1983, table 3, these lines are named $\boldsymbol{B_3}$ G-M Lines. They characterize a two-fold screw axis $\mathbf{2_1}$ parallel to **c** axis. Since the point group has been proved to be **mmm,** the ***00l*** reflections, with ***l*** odd, which appear in the FOLZ ring, are linear oriented and parallel to **c*** axis. Thus, this shows that a sliding mirror plan ***c*** perpendicular to [010] exists.

From the carried out investigation, the space group $\mathbf{C2/m2/}\boldsymbol{c}\mathbf{2_1/m}$ (**C*m*cm**) number 63 of International Tables for Crystallography has been deducted.

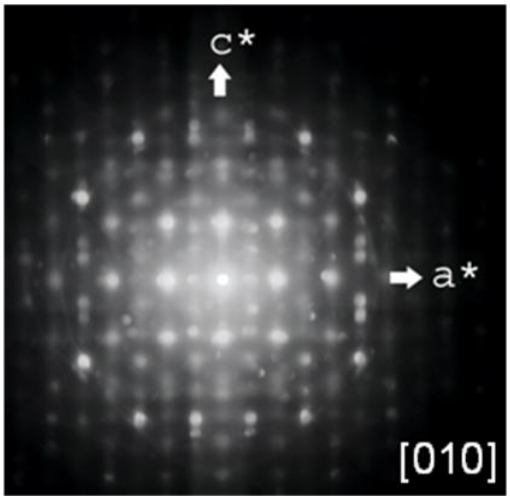

Figure . CBED pattern of zone axis [010] showing the B_3 G-M lines in the forbiden reflections parallel to c*.

Table 3. G-M line for the point group **mmm** of C lattice from Tanaka et al. 1983

Space group	Incident beam direction [100]		[010]		[001]	[hk0]		[0kl]		[h0l]	
63 $C2/m2/c2_1/m$	$00l$ $c,2_1$	A_2B_2 A_3B_3	$00l$ 2_1	B_3		$00l$ 2_1	A_2B_2 B_3			$0k'l'$ c	A_2B_2 A_3
64 $C2/m2/c2_1/a$	$00l$ $c,2_1$	A_2B_2 A_3B_3	$00l$ 2_1	B_3		$h'k'0$ a $00l$ 2_1	A_2B_2 A_3 A_2B_2 B_3			$0k'l'$ c	A_2B_2 A_3
65 $C2/m2/m2/m$											
66 $C2/c2/c2/m$	$00l$ c_2	A_3	$00l$ c_1	A_3				$0k'l'$ c_1	A_2B_2 A_3	$0k'l'$ c_2	A_2B_2 A_3
67 $C2/m2/m2/a$						$h'k'0$ a	A_2B_2 A_3				
68 $C2/c2/c2/c$	$00l$ c_2	A_3	$00l$ c_1	A_3		$h'k'0$ a	A_2B_2 A_3	$0k'l'$ c_1	A_2B_2 A_3	$h'0l'$ c_2	A_2B_2 A_3

4. Conclusion and discussion

Single crystal of the new homologous phase $Ga_2O_3(ZnO)_{10}$ has been synthesized. Phase and Symmetry determination have been performed by the means of CBED technique. Previous investigations by the means of X-Ray diffraction on powder of homologous series **$Ga_2O_3(ZnO)_m$(*m*=7, 8, 9, 11, 16)** showed that these substances crystallized in the space group **Cmcm** (Kimizuka et al. 1995). Later, another Studies by the means of SAD (selected area diffraction) on new homologous phases $Ga_2O_3(ZnO)_9$ and $Ga_2O_3(ZnO)_{13}$ pretended that the homologous series with chemical composition **$Ga_2O_3(ZnO)_m$(m>8)** belong to the space group **$Cmc2_1$** (Chunfei Li et al. 1999).

The space groups **Cmcm** and **$Cmc2_1$** are characterized by the same cinematic extinction law. However, these space groups can be respectively distinguished by the existence or the lack of the symmetry centre. Since the respective extinction rules do not give any information to the question of symmetry centre, the new homologous phase, $Ga_2O_3(ZnO)_{10}$, has been investigated and characterized by the means of CBED technique.

To summarize, firstly, the main zone axes ([100], [010] and [001]) and the corresponding lattice parameters (a=3.32, b=19.45, c=36.55 Å, and α=β=γ=90˚) have been determined. Secondly, the Bravais lattice (**C**-centred) and thirdly, the point group (**mmm**) and the space group (**Cmcm**) from the reciprocity theorem and the dynamic extinction rule. The determined symmetry agrees with the declaration that compounds belonging to the $\mathbf{Ga_2O_3(ZnO)_m}$ homologous series have orthorhombic symmetry (Michiue Y. et al. 2012).

Acknowledgements. The Department of inorganic chemistry at the University of Bonn in Germany is thanked for supporting this study.

References

B. F. Buxton; J. A. Eades; J. W. Steeds; G. M. Rackham. Philosophical Transactions of the Royal Society of London. Series A, Mathematical and Physical Sciences, Vol., **281**, No 1301(Mar. 11, 1976), 171-194.

C. Campbell, Surface Acoustic Wave Devices and Their Signal Processing. Applications (Academic Press, San Diego, 1989)

Chunfei Li, Yoshio Bando, Masaki Nakamura, Keiji Kurashima and Noboru Kimizuka, Acta Cryst. (1999). **B55**, 355-362

Cowley, J. M. & Moodie, A. F. (1959). Acta Cryst. **12**, 360.

D.M. Bird, Journal of electron microscopy technique **13**:77-97(1989)

D. S. Ginley, C. Bright, Mater. Res. Soc. Bull. **25** (2000) 15-21

Goodman, P. & Lehmpfuhl, G. (1968). Acta Cryst**. A24**, 339-347.

H. Cao, J. Y. Xu, D. Z. Zhang, S. H. Chang, S. T. Ho, E. W. Seelig, X. Liu, R. P. H. Chang, Phys. Rev. Lett. **84** (2000) 5584-5587.

J. GjØnnes and A. F. Moodie. Acta Cryst. (1965).

J.M. Zuo, Ultramicroscopy, vol. **41**, (1989), pp. 223

J. M. Howe. Acta Cryst. (1986). **A42**, 368-380

J. W. Steeds and R. Vincent. J. Appl. Cryst. (1983). **16**, 317-324

Kasper, H. (1967). Z. Anorg. Allg. Chem. **349**, 113-123

Kimizuka, N., Isobe, M., Nakamura, M.& Mohri, T. (1993). J. Solid Stade Chem. **103**, 394-402

Kimizuka, N., Mohri, T. & Nakamura, M. (1989). J. Solid State Chem. **81**, 70-77

Kimizuka, N., Isobe, M. & Nakamura, M. (1995). J. Solid State Chem. **116**, 170-178

Kluwer Academic Publishers, Dordrecht /Boston /London. The InternationalTables for Crystallography Volume **A** (1992)

Kudo A. & Mikami, I. (1998) Chem. Lett. pp. 1027-1028

M. Tanaka, H. Sekii and T. Nagasawa. Acta Cryst. (1983). **A39**, 825-837

M. Tanaka and M. Terauchi CBED, JEOL Ltd., Tokyo (1985)

M. Tanaka, M. Terauchi CBED II, JEOL Ltd., Tokyo (1988)

M. Tanaka, R. Saito and H. Sekii. Acta Cryst. (1983). **A39**, 357-368.

M. Tanaka, Journal of electron microscopy technique **13**:27-39(1989)

M. Tanaka, H. Sekii and T. Nagasawa. Acta Cryst. (1983). **A 39**, 825-837.

Michiue Y., Noboru Kimizuka, Yasushi Kanke and Takao Mori, Acta cryst. (2012) **B68**, 250-260

Michiue, Y. & Kimizuka, N. (2010). Acta Cryst. **B66**, 117-129

Michiue, Y., Kimizuka, N. & Kanke, Y. (2008). Acta Cryst. B64, 521-526

Michiyoshi Tanaka, J. Electron Microsc., Vol. **35**, No. 4, 314- 323, 1986

Michiyoshi Tanaka, Ryuichi Saito, Katsuyoshi Ueno and Yoshiyasu Hrada, J. Electron Microsc., No. **4**, 408-412, 1980

Michiyoshi Tanaka, Acta Cryst. (1994). **A50**, 261-286

Moriga, T., Edwards, D. D., Mason, T. O., Palmer, G. B., Poeppelmeier, K. R., Schindler, J. L., Kannewurf, C. R. & Nakabayashi, I. (1998). J. Am. Ceram. Soc. **81**, 1310-1316

P. Goodman (1975). Acta Cryst. **A31**, 804-810.

P. Goodman and H. J. Whitfield. Acta Cryst. (1980). **A36**, 219-228

Pogany, A.P., and Turner, P.S. (1968) Acta Cryst., **A24**: 103-109.

Raghavan Ayer. (1989) Journal of Electron Microscopy Technique **13**:16-26

Steeds, J. W. (1980). Electron Microscopy 4, Antwerp, **1980**, pp. 96-103

T. Minami, H. Nanto and S. Tanaka, Jpn. J. Appl. Phys**. 23**, L 280 (1984)

Y. G. Wang, C. Yuen, S. P. Lau, S.F. Yu, B. K. Tay, Chem. Phys. Lett. **377** (2003) 329